Tricellulin regulates the tight junctions and cytoskeleton of pancreatic acinar cells through the NF-κB pathway in hypertriglyceridemic acute pancreatitis

GUIFANG WEI[1], ZHENNI LIANG[1], HAIXING WEI[1], QING WU[1], JIE WANG[1], LIANJIE LIN[2], ZHIHAI LIANG[2], HUIYING YANG[2] and MENGBIN QIN[1]

[1]Department of Gastroenterology, The Second Affiliated Hospital of Guangxi Medical University, Nanning, Guangxi Zhuang Autonomous Region 530007, P.R. China; [2]Department of Gastroenterology, The First Affiliated Hospital of Guangxi Medical University, Nanning, Guangxi Zhuang Autonomous Region 530021, P.R. China

Received March 3, 2026; Accepted May 7, 2026

DOI: 10.3892/br.2026.2160

Abstract. Hypertriglyceridemic acute pancreatitis (HTGAP) is a clinical emergency. Tight junctions (TJs) and the cytoskeleton are essential for cell-cell junctions and cell survival, and although tricellulin is a key protein regulating cell junctions, its role in regulating TJ proteins and the cytoskeleton in pancreatic acinar cells in HTGAP is not currently clear. In the present study, 24 female hamsters were assigned to the control, hypertriglyceridemia (HTG), HTGAP and HTGAP + SC75741 groups. HTG was induced by a high-fat diet and HTGAP was established by retrograde sodium taurocholate injection. Serum triglyceride levels, pancreatic histopathological changes, and pancreatic expression of tricellulin, claudin-1 and NF-κB p65 were assessed. Furthermore, AR42J cell models with tricellulin overexpression and knockdown were cultured under HTG conditions, and protein levels were semi-quantified by western blotting. F-actin organization was assessed by immunofluorescence staining and intercellular morphology was examined by scanning electron microscopy. The results revealed that tricellulin expression was decreased and p65 expression was increased under hypertriglyceridemic conditions, whereas pancreatic histopathological injury was not significantly increased in the HTG group. The HTGAP group showed significantly more severe pancreatic injury than the control and HTG groups, accompanied by significantly decreased tricellulin and claudin-1 expression, and significantly increased p65 expression. After SC75741 (an inhibitor of the NF-κB signaling pathway) treatment, pancreatic injury and p65 expression were significantly decreased, whereas tricellulin and claudin-1 showed only partial recovery. In AR42J cells, tricellulin overexpression was associated with increased claudin-1 expression, reduced NF-κB activation, improved F-actin organization and better-preserved intercellular morphology, whereas tricellulin knockdown exhibited the opposite pattern. In conclusion, hypertriglyceridemic conditions were associated with impaired TJ integrity and cytoskeletal disorganization in pancreatic acinar cells, accompanied by reduced tricellulin expression and increased NF-κB activation. These findings suggest that tricellulin may contribute to HTGAP-related junctional and cytoskeletal injury, potentially involving NF-κB signaling.

Correspondence to: Dr Mengbin Qin, Department of Gastroenterology, The Second Affiliated Hospital of Guangxi Medical University, 166 Daxuedong Road, Nanning, Guangxi Zhuang Autonomous Region 530007, P.R. China
E-mail: dr.mmbin@hotmail.com

Key words: hypertriglyceridemic acute pancreatitis, tricellulin, cytoskeleton, NF-κB pathway, hamster model

Introduction

Acute pancreatitis (AP) is a common clinical emergency with a worldwide rising incidence. Hypertriglyceridemia (HTG) is the third most common cause of AP and accounts for ~22% of all AP cases, following gallstone disease and alcohol consumption (1,2). HTG should be distinguished from hypertriglyceridemic AP (HTGAP); HTG refers to a metabolic condition characterized by elevated serum triglyceride (TG) levels, whereas HTGAP refers to AP occurring in the setting of HTG. Patients with HTGAP usually experience a more severe clinical course and more complications than patients with AP without HTG (3-5). Animal experiments have shown that HTGAP can aggravate the pancreatic and systemic inflammatory response, including infection and multiple organ failure (6). However, it is still not fully clear how HTG impacts the course of AP. Under hypertriglyceridemic conditions, excessive TGs can be hydrolyzed into free fatty acids (FFAs), which may induce inflammatory activation, membrane injury, calcium dysregulation and acinar cell damage (7).

Because epithelial barrier integrity and intercellular junction stability are important for maintaining tissue homeostasis, disruption of tight junction (TJ) architecture may contribute to pancreatic injury under HTG conditions (8). The TJ is an important intercellular ultrastructure that selectively regulates the permeability of small molecules and ions between cells.

TJs restrict and regulate the free diffusion of solutes through the paracellular pathway in epithelial cells and contribute to the establishment of distinct body fluid compartments, termed the barrier function (9). TJs are classified into bicellular TJs (bTJs) and tricellular TJs (tTJs). Occludin and claudins are the main constituents of bTJ proteins involved in the formation and maintenance of epithelial barriers, whereas tricellulin and angulins are the main components of tTJs (10-12). During inflammation, which is known to decrease the levels of occludin and claudins in bTJs, tricellulin can move to bTJs to maintain their integrity (13). Long-term stimulation by numerous FFAs can lead to the contraction of epithelial cells, decreasing intercellular TJs (14). HTG downregulates the levels of tTJ proteins in the pancreatic ductal mucosal barrier and increases the severity of pancreatitis (9). However, the role of HTG in pancreatic acinar cells is still not clear.

Tricellulin, encoded by the Marveld2 gene, is a protein exclusively localized at tTJs, which provides a basis for various epithelial stereo-structures (15) and regulates the junctional tension of epithelial cells (16). However, its molecular function remains to be fully understood. In the pancreas, tricellulin is highly expressed in the ducts and acini at tricellular contacts (17). Studies using both *in vitro* (18) and *in vivo* HTGAP rat models (9), have shown that HTG impairs the TJ structure of the biliary-pancreatic duct. The cytoskeleton is a reticular structure essential for cell survival and microfilaments are crucial for the secretion of intracellular substances (19). The pancreatic tissue of mice with HTGAP shows an increased activation of the NF-κB signaling pathway (20), which is involved in the regulation of functions of microfilaments and the cytoskeleton (21). Although tricellulin reduces apoptosis through the NF-κB signaling pathway in colorectal cancer cells (22), its role in the regulation of TJ proteins and the cytoskeleton in pancreatic acinar cells in HTGAP is not fully understood.

The present study hypothesized that hypertriglyceridemic conditions may impair TJ integrity and cytoskeletal organization in pancreatic acinar cells, and that tricellulin could contribute to this process in association with NF-κB signaling. To test this hypothesis, a hamster model of HTGAP and HTG-treated AR42J cells with tricellulin overexpression or knockdown were used. Subsequently, pancreatic injury, tricellulin and claudin-1 expression, NF-κB activation, F-actin organization and TJ ultrastructure were assessed.

Materials and methods

Animals and experimental design. A total of 24 female hamsters (age, 3 weeks; body weight, 60-70 g) were acquired from Shanghai Yanji Bio-tech Co., Ltd. The animals were housed in a facility maintained at 24˚C under a 12-h light/dark cycle, and were given free access to water and chow. The present study was carried out in accordance with the recommendations of the animal protection guidelines approved by the local animal ethics committee. The study protocol was approved by the Ethics Committee for Medical Experimental Animals, Second Affiliated Hospital of Guangxi Medical University [approval no. 2022(KY-0174); Nanning, China].

The hamsters were randomly divided into the following four groups: Control group (n=6), HTG group (n=6), HTGAP group (n=6), and HTGAP + SC75741 group (n=6). No direct comparison between male and female hamsters was performed; therefore, sex-specific differences could not be assessed and should be addressed in future studies. Hamsters in the HTG, HTGAP and HTGAP + SC75741 groups were fed a high-fat diet (82.8% normal chow + 15% saturated animal fat + 2% cholesterol + 0.2% sodium cholate), whereas hamsters in the control group were fed standard hamster chow.

After the animals were fed standard hamster chow or a high-fat diet for 5 weeks, 0.1-0.2 ml blood was collected from the retro-orbital vein and centrifuged at 1,000 x g for 15 min at 4˚C to isolate serum. Subsequently, serum TG levels were measured to confirm successful establishment of the HTG model using a TG Fluorometric Assay Kit (cat. no. E-BC-F033; Elabscience Bionovation Inc.) according to the manufacturer's instructions. HTG induction was confirmed when serum TG levels in the experimental group were >2-fold higher than those in the control group. The HTGAP model was established by retrograde injection of 6% sodium taurocholate (TCI Tokyo Chemical Industry Co., Ltd.) into the bile and pancreatic duct under isoflurane anesthesia; anesthesia was induced with 5% isoflurane and maintained at 3-4% during the surgical procedure, with reference to established rodent inhalation anesthesia protocols (23). Sodium taurocholate was infused at a volume of 0.1 ml/100 g body weight and a rate of 0.1 ml/min using an infusion pump. Successful cannulation and injection were confirmed by visual observation of pancreatic duct dilatation. The common bile duct was not clamped during the procedure. Sham-operated controls were not included in the present study. The hamsters in the HTGAP + SC75741 group were treated with SC75741 (MedChemExpress), an inhibitor of the NF-κB signaling pathway, through intraperitoneal injection (1 mg/100 g body weight) 30 min before modeling (24). All of the animals were fasted for 6 h before surgical operations. After 24 h of AP induction, euthanasia was performed via intraperitoneal injection of an overdose of pentobarbital sodium (200 mg/kg), in accordance with the approved animal protocol and supporting rodent euthanasia literature (25,26). No hamsters died during anesthesia; however, one hamster in the HTGAP group died unexpectedly during postoperative recovery from anesthesia after model induction. Humane endpoints included severe respiratory distress, inability to eat or drink, persistent recumbency or a moribund appearance; no animals were euthanized early before the planned endpoint. Subsequently, 2-3 ml blood was collected from the abdominal aorta and centrifuged at 1,000 x g for 15 min at 4˚C, and the serum was conserved at -80˚C. Pancreatic tissues used in the present study were fixed in 10% formalin at room temperature for 24 h, embedded in paraffin, and used for histopathological and immunohistochemical analyses. Finally, the animal carcasses were uniformly sent to the Guangxi Zhuang Autonomous Region Hazardous Waste Disposal Center for processing.

Study endpoints. The primary study endpoints were pancreatic injury, and changes to the expression levels of tricellulin, claudin-1 and NF-κB pathway-related proteins. Secondary endpoints included F-actin cytoskeletal organization and intercellular morphological changes, and alterations in cell-cell contacts in AR42J cells.

Table I. Primer sequences used for reverse transcription-quantitative PCR.

Gene	Forward primer, 5'-3'	Reverse primer, 5'-3'
Marveld2	ACGATTATTATCCTGGTGCTTG	ACCTCGGTTGGTATCATTCA
GAPDH	GGCAAGTTCAACGGCACA	TCTCGCTCCTGGAAGATGG

Histopathological analysis. The pancreatic specimens were cut into 3-μm sections and subjected to hematoxylin and eosin staining. Sections were stained with hematoxylin for 2 min, differentiated with 1% hydrochloric acid alcohol for 30 sec and counterstained with eosin for 30 sec, all at room temperature. Pancreatic injury was assessed according to a previously reported scoring system, including edema, inflammatory cell infiltration, hemorrhage and necrosis (27). Morphology was assessed under a light microscope and histopathological evaluation was performed independently by two investigators blinded to group allocation.

Immunohistochemical analysis. Formalin-fixed, paraffin-embedded pancreatic tissue sections were deparaffinized, and antigens were retrieved through high-pressure cooking with citrate buffer (pH 6.0) for 5 min. Subsequently, these tissue sections were subjected to gradient cooling until they reached room temperature and were then washed thoroughly in phosphate-buffered saline (PBS; pH 7.4). The sections were quenched with 3% hydrogen peroxide for 30 min at room temperature, blocked with 3% bovine serum albumin (Beijing Solarbio Science & Technology Co.) at room temperature for 15 min, and incubated overnight at 4˚C with primary antibodies against tricellulin (1:500; cat. no. 13515-1-AP), claudin-1 (1:500; cat. no. 13050-1-AP) and NF-κB p65 (1:300; cat. no. 10745-1-AP) (all from Wuhan Sanying Biotechnology). The next day, the tissue sections were washed and incubated with HRP-based secondary antibody reagents using an SABC-HRP Kit with Anti-Rabbit IgG (IHC&ICC) (cat. no. P0615; Beyotime Biotechnology) for 15 min at room temperature. The slides were then placed in PBS, washed three times on a decolorizing shaker (5 min/wash) and visualized with DAB (50 μl/slide; Beijing Zhongshan Jinqiao Biotechnology Co., Ltd.). Images were acquired using a pathology image analysis system (Leica DMR+Q550; Leica Microsystems GmbH) under identical settings, and quantitative analysis was performed using Image-Pro Plus 6.0 (Media Cybernetics, Inc.). Three randomly selected non-overlapping fields per section were analyzed and quantification was performed in a blinded manner.

Cell culture, infection and treatment. The rat pancreatic exocrine cell line AR42J (RRID: CVCL_0143) was obtained from the American Type Culture Collection and cultured to an appropriate density in Dulbecco's Modified Eagle Medium (Gibco; Thermo Fisher Scientific, Inc.) supplemented with 10% fetal bovine serum (Gibco; Thermo Fisher Scientific, Inc.) in a humidified incubator containing 5% CO_2 at 37˚C. Three tricellulin short hairpin (sh)RNAs were designed and evaluated for lentiviral knockdown experiments: sh1, 5'-GGATAAGCC AGTGTCAGAT-3'; sh2, 5'-GCTTGGATCGCGACGATTA-3'; and sh3, 5'-GCCACATTCCTAAGCCCAT-3'. A non-targeting negative control shRNA sequence (5'-CCTAAGGTTAAG TCGCCCTCG-3') was used as the control. The lentiviral shRNA vector and the corresponding control vector were commercially constructed and packaged by OBiO Technology (Shanghai) Corp., Ltd., and were based on pSLenti-U6-shRNA (Marveld2)-CMV-EGFP-F2A-Puro-WPRE. In addition, a lentiviral overexpression vector carrying tricellulin and the corresponding control vector were also commercially constructed and packaged by OBiO Technology (Shanghai) Corp., Ltd.; these were based on pcSLenti-EF1-EGFP-P2 A-Puro-CMV-Marveld2-3xFLAG-WPRE. The efficiency of tricellulin knockdown and overexpression was validated in AR42J cells infected with these lentiviral constructs alone by reverse transcription-quantitative PCR (RT-qPCR) (Fig. S1). For lentiviral infection, AR42J cells were seeded in 6-well plates at $5x10^5$ cells/well and infected at a multiplicity of infection of 100 in the presence of polybrene (10 μg/ml) at 37˚C. After 8 h, the medium was replaced with complete medium and stable cell lines were selected using puromycin (5 μg/ml) until harvest. Cells were harvested 72 h after infection for RT-qPCR validation. Briefly, total RNA was extracted from lentivirus-infected AR42J cells using RNAiso Plus (cat. no. 9109; Takara Bio, Inc.). RT was performed using an RT kit (cat. no. K1622; Thermo Fisher Scientific, Inc.) according to the manufacturer's protocol. qPCR was performed using SYBR Green Mix (cat. no. 11201ES60; Shanghai Yeasen Biotechnology Co., Ltd.) on a BIOER 9600 Plus real-time PCR system (Bioer Technology Co., Ltd.). Thermocycling was performed as follows: Initial denaturation at 95˚C for 5 min, followed by 40 cycles at 95˚C for 10 sec and 60˚C for 30 sec. Relative mRNA expression was quantified using the $2^{-\Delta\Delta Cq}$ method (28). The primer sequences used for RT-qPCR, including the internal control GAPDH, are listed in Table I.

To determine the effects of tricellulin on AR42J cells in the HTG environment, lentivirus-infected cells were treated with 66-μM palmitic acid (MilliporeSigma) + 132-μM oleic acid (MilliporeSigma) for 24 h at 37˚C for subsequent experiments. To explore the effects of the NF-κB pathway on AR42J cells, lentivirus-infected cells were treated with 1 μM SC75741 for 24 h at 37˚C for subsequent experiments. Cells cultured without any extra reagents were regarded as the control group. Unless otherwise stated, *in vitro* experiments were performed in three independent biological replicates.

Western blotting. Cultured cells were lysed in RIPA lysis buffer (Beijing Solarbio Science & Technology Co., Ltd.) and protein concentrations were determined by BCA assay. Total protein samples (20 μg) were then separated by SDS-PAGE on 10% and transferred to a polyvinylidene difluoride membrane. After blocking with 5% non-fat milk for 1 h at room temperature, the

Table II. Serum TG levels, histopathological scores, and immunohistochemical expression of tricellulin, claudin-1 and p65 in the pancreatic tissues of hamsters.

				AOD value		
Group	N	TG, mmol/l	Histological score	Tricellulin	Claudin-1	p65
C	6	1.68±0.18	0.5 (0.0-1.0)	0.27±0.02	0.28±0.03	0.14±0.02
HTG	6	4.85±0.79[a]	1.0 (0.25-1.0)	0.22±0.01[a]	0.29±0.01	0.16±0.01
HTGAP	6	4.33±1.42[a]	7.0 (7.0-7.75)[a,b]	0.17±0.02[a,b]	0.22±0.01[a,b]	0.27±0.02[a,b]
HTGAP + SC75741	6	4.93±1.91[a]	5.0 (4.25-5.0)[a-c]	0.19±0.02[a,b]	0.23±0.02[a,b]	0.23±0.01[a-c]

[a]P<0.05 vs. C group; [b]P<0.05 vs. HTG group; [c]P<0.05 vs. HTGAP group. Histological scores are presented as the median (IQR) and were analyzed using the Kruskal-Wallis test followed by Bonferroni-corrected pairwise Mann-Whitney U tests. All other data are presented as the mean ± SD. Parametric data were analyzed using one-way ANOVA followed by Tukey's post hoc test, or Welch's ANOVA followed by Dunnett's T3 test when homogeneity of variance was not met. AOD, average optical density; C, control; HTG, hypertriglyceridemia; HTGAP, hypertriglyceridemic acute pancreatitis; TG, triglyceride.

membranes were incubated with primary antibodies against β-actin (1:20,000; cat no. 66009-1-Ig), tricellulin (1:1,000; cat. no. 13515-1-AP), claudin-1 (1:1,000; cat. no. 13050-1-AP), NF-κB p65 (1:1,000; cat. no. 10745-1-AP) and NF-κB phosphorylated-p65 (p-p65; 1:2,000; cat. no. 82335-1-RR) (all from Wuhan Sanying Biotechnology) overnight at 4˚C. Subsequently, the membrane was washed three times with Tris-buffered saline-0.1% Tween-20 buffer and incubated for 60 min at room temperature with HRP-conjugated secondary antibodies, including Peroxidase AffiniPure® Goat Anti-Rabbit IgG (H+L) (1:50,000; cat. no. 111-035-003; Jackson ImmunoResearch) and Peroxidase AffiniPure Goat Anti-Mouse IgG (H+L) (1:50,000; cat. no. 115-035-003; Jackson ImmunoResearch), as appropriate. Protein bands were visualized using Tanon™ Femto-sig ECL chemiluminescent substrate (cat. no. 180-506; Tanon Science and Technology Co., Ltd.) and semi-quantified using Quantity One software (version 4.6.0; Bio-Rad Laboratories, Inc.).

Immunofluorescence staining of F-actin. Cells were plated onto coverslips (24x24 mm) in 6-well plates until they reached 55-60% confluency. The cells were then fixed in 4% paraformaldehyde for 15 min at room temperature, permeabilized in 0.1% Triton X-100 for 5 min at room temperature, blocked in PBS containing 2% bovine serum albumin for 20 min at room temperature and stained with tetramethyl rhodamine isothiocyanate-phalloidin (100 nM; 50 μl/well; Beijing Solarbio Science & Technology Co., Ltd.) for 30 min at room temperature in the dark. The samples were washed with PBS three times at 5-min intervals between each step and mounted with an anti-fading medium containing DAPI (Beijing Solarbio Science & Technology Co., Ltd.) for 3 min at room temperature in the dark. F-actin was visualized at 530-550 nm and cell nuclei were observed at 460-495 nm under an upright fluorescence microscope (BX53; Olympus Corporation).

Scanning electron microscopy. The intercellular TJ ultrastructure of AR42J cells was evaluated by scanning electron microscopy. Cells were washed with PBS and fixed in 3% glutaraldehyde at 4˚C for >2 h, followed by post-fixation in 1% osmium tetroxide. After the cells were dehydrated through a graded ethanol series, samples were dried, mounted on metal stubs, sputter-coated with gold and examined using a scanning electron microscope (H-7650; Hitachi, Ltd.).

Statistical analyses. Data are presented as the mean ± standard deviation. Normality was assessed using the Shapiro-Wilk test and homogeneity of variance was assessed using Levene's test. For comparisons among multiple groups, one-way analysis of variance was used when parametric assumptions were met, followed by Tukey's post hoc test. Welch's ANOVA followed by Dunnett's T3 test was applied when homogeneity of variance was not met. Because histological scores are ordinal data, they are presented as the median (IQR) and were analyzed using the Kruskal-Wallis test followed by Bonferroni-corrected pairwise Mann-Whitney U tests. Comparisons between two groups were performed using an unpaired Student's t-test. Unless otherwise stated, *in vitro* experiments were performed in three independent biological replicates. P<0.05 was considered to indicate a statistically significant difference. Statistical analyses were performed using SPSS 20.0 (IBM Corp.).

Results

Serum TG values. Serum collected from the hamsters in the high-fat diet groups (HTG, HTGAP and HTGAP + SC75741 groups) was lipemic on visual inspection, whereas that of the control group was clear. Serum TG levels differed significantly among the groups (P=0.001). Serum TG levels in the HTG, HTGAP and HTGAP + SC75741 groups were all significantly higher than those in the control group (P=0.001, P=0.027 and P=0.039, respectively), confirming successful induction of HTG (Table II). No significant difference was observed among the HTG, HTGAP and HTGAP + SC75741 groups (all P>0.05).

Macroscopic view and histopathological analysis of the pancreas. On macroscopic examination, pancreatic edema, hemorrhage and necrosis were observed mainly in the HTGAP and HTGAP + SC75741 groups (Fig. 1A). In the HTG group, the pancreas showed no obvious necrosis or hemorrhage on gross examination, and only minimal or no histopathological

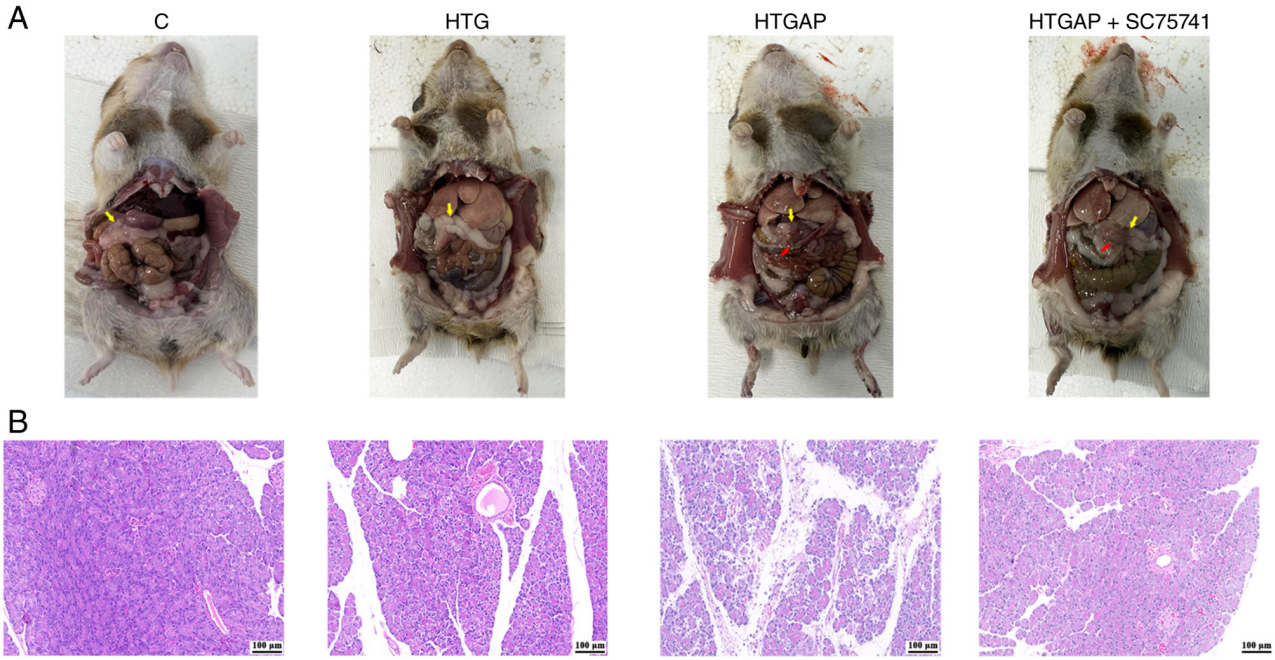

Figure 1. Macroscopic and histopathological changes in the pancreas of hamsters. (A) Representative macroscopic appearance of the pancreas in each group. Yellow arrows indicate the pancreas; red arrows indicate necrotic areas. (B) Representative hematoxylin and eosin staining of pancreatic tissues from each group (magnification, x200; scale bars, 100 μm). C, control; HTG, hypertriglyceridemia; HTGAP, hypertriglyceridemic acute pancreatitis.

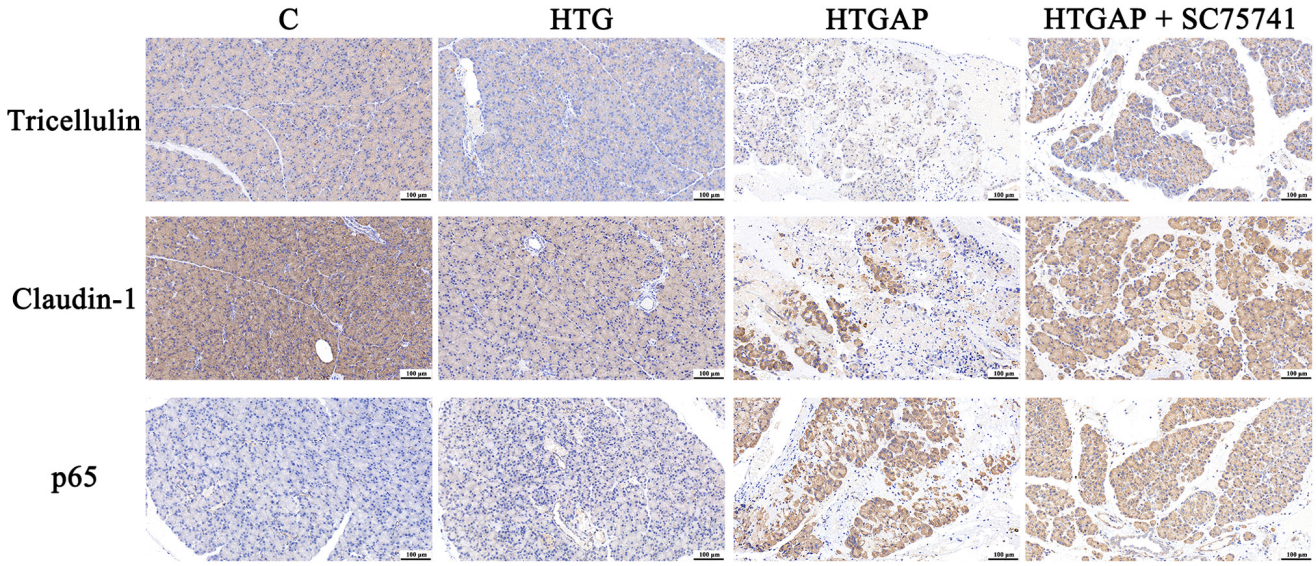

Figure 2. Representative immunohistochemical staining of tricellulin, claudin-1 and NF-κB p65 in pancreatic tissues from hamsters in different groups (magnification, x200; scale bars, 100 μm). C, control; HTG, hypertriglyceridemia; HTGAP, hypertriglyceridemic acute pancreatitis.

abnormalities were observed. Notably, the necrotic lesions were mainly concentrated in the head of the pancreas. Occasional biliary fistula and scattered calcification foci were observed in the HTGAP group, but these findings were not predefined endpoints and were not quantitatively analyzed. Histologically, the control group exhibited no obvious edema, inflammatory infiltration or necrosis, whereas the HTGAP and HTGAP + SC75741 groups showed evident edema, inflammatory infiltration, hemorrhage and necrosis (Fig. 1B). Histopathological scores differed significantly among the groups (Kruskal-Wallis test, P<0.001). After Bonferroni-corrected pairwise comparisons, the HTGAP group showed significantly higher pathological scores than the control and HTG groups (both P<0.05) (Table II). The HTGAP + SC75741 group also showed significantly higher pathological scores than the control and HTG groups (both P<0.05), but significantly lower scores than the HTGAP group (P=0.002). No significant difference was observed between the control and HTG groups (P=0.846).

Effects of HTG on the expression of TJ proteins and NF-κB pathway activation in pancreatic tissues. Immunohistochemical analysis showed significant group

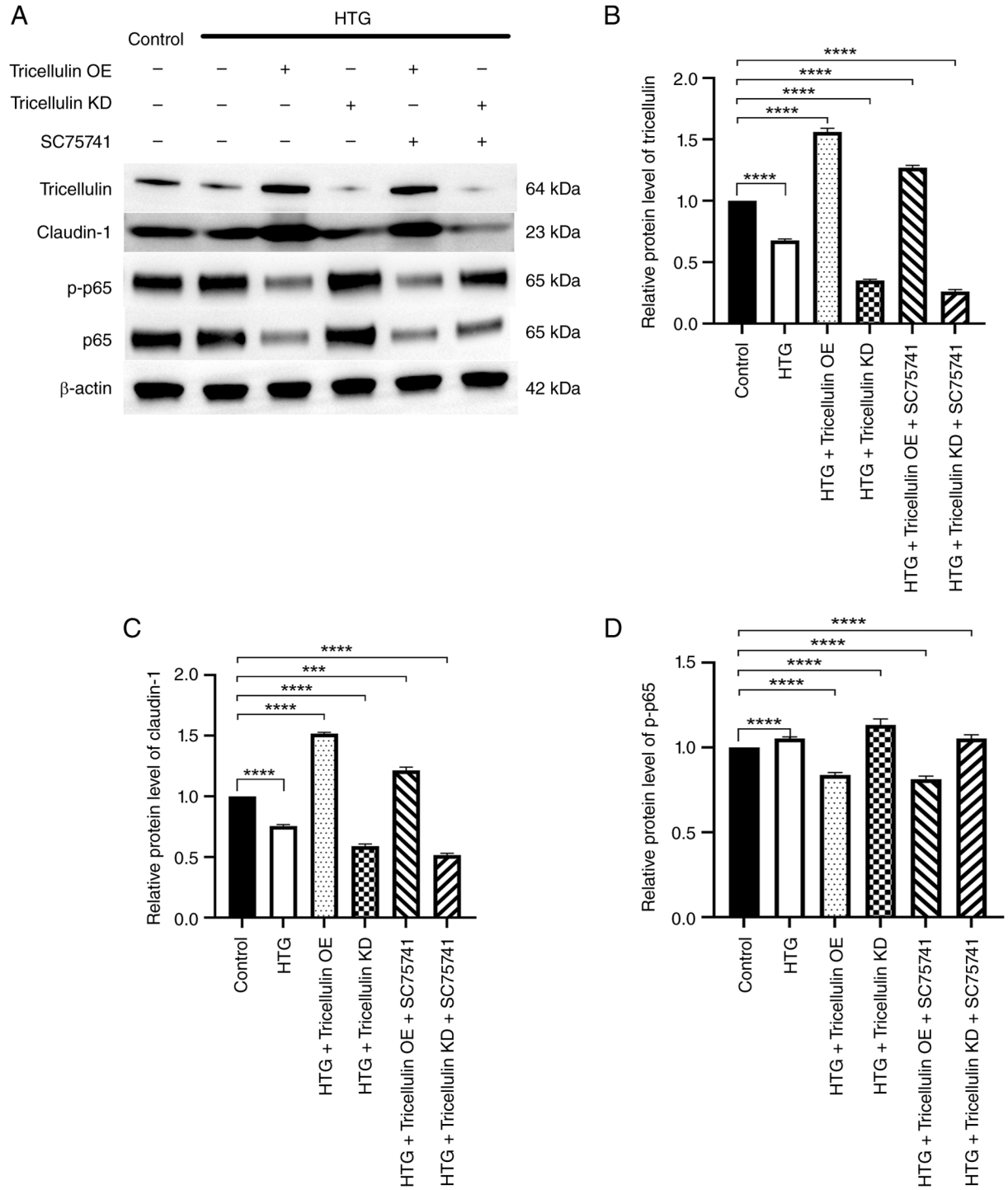

Figure 3. Effects of tricellulin modulation and NF-κB inhibition on tight junction proteins and NF-κB signaling in AR42J cells under an HTG environment. (A) Representative western blot analysis of tricellulin, claudin-1, p-p65, total p65 and β-actin. Densitometric semi-quantification of (B) tricellulin, (C) claudin-1 and (D) p-p65 normalized to β-actin or total p65, as appropriate. Data are presented as the mean ± SD of three independent biological replicates. ***P<0.001; ****P<0.0001. HTG, hypertriglyceridemia; KD, knockdown; NC, negative control; OE, overexpression; p-, phosphorylated.

differences in tricellulin, p65 and claudin-1 expression (Fig. 2; Table II). For tricellulin, the overall difference among groups was significant (P<0.05), and Tukey's post hoc test showed that tricellulin expression was significantly lower in the HTG, HTGAP and HTGAP + SC75741 groups than in the control group (P=0.001, P<0.05 and P<0.05, respectively). In addition, tricellulin expression in the HTGAP group was significantly lower than that in the HTG group (P=0.001), whereas no significant difference was observed between the HTGAP and HTGAP + SC75741 groups (P=0.519).

For p65, the overall difference among groups was also significant (P<0.05). Tukey's post hoc analysis showed that p65 expression was significantly higher in the HTGAP group than in the control, HTG and HTGAP + SC75741 groups (all P<0.05). The HTGAP + SC75741 group also showed significantly higher p65 expression than the control and HTG groups

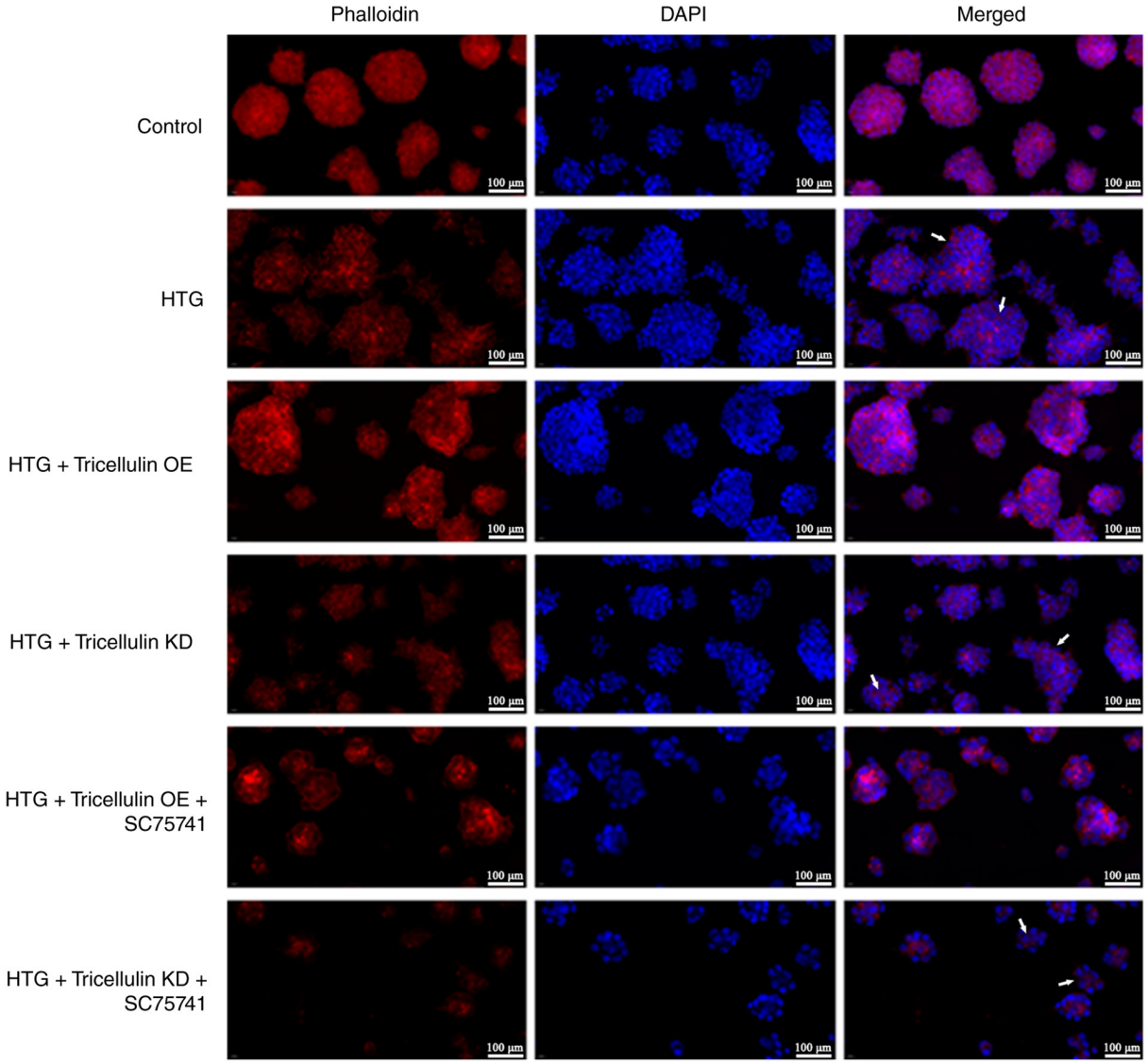

Figure 4. Representative images of immunofluorescence analysis of F-actin organization after tricellulin modulation and SC75741 treatment in AR42J cells. F-actin is stained with phalloidin (red), and nuclei are stained with DAPI (blue). White arrows indicate representative areas of reduced F-actin continuity, weaker cortical distribution and a disorganized filament pattern. Scale bars, 100 μm. HTG, hypertriglyceridemia; KD, knockdown; NC, negative control; OE, overexpression.

(both P<0.05), whereas no significant difference was found between the control and HTG groups (P=0.290).

For claudin-1, the overall difference among groups was significant (P<0.05). Because the homogeneity of variance assumption was not satisfied, Dunnett's T3 test was used for pairwise comparisons. Claudin-1 expression was significantly lower in the HTGAP group than in the control group (P=0.008) and the HTG group (P<0.05). The HTGAP + SC75741 group also exhibited significantly lower claudin-1 expression than the control group (P=0.016) and the HTG group (P<0.05). No significant difference was observed between the HTGAP and HTGAP + SC75741 groups (P=0.877), nor between the control and HTG groups (P=0.894). These findings indicated that claudin-1 reduction was mainly observed after AP induction rather than under HTG alone.

Effect of regulating tricellulin and the NF-κB pathway on the expression of TJ proteins and activation of the NF-κB pathway in AR42J cells in the HTG environment. RT-qPCR validation in AR42J cells transduced with lentiviral constructs alone showed marked upregulation of Marveld2 mRNA in the overexpression group, whereas among the three shRNAs tested, sh1 showed the strongest knockdown efficiency compared with the corresponding negative controls (Fig. S1). The expression levels of tricellulin, claudin-1, and NF-κB p-p65 and total p65 were analyzed by western blotting. The expression levels of tricellulin and claudin-1 were decreased, whereas those of NF-κB p-p65 slightly increased under HTG conditions relative to the baseline values. Total p65 expression showed only modest variation across groups, with lower levels in the tricellulin overexpression and tricellulin overexpression + SC75741 groups, whereas the tricellulin knockdown group remained close to the HTG group (Fig. 3). Overexpression of tricellulin upregulated claudin-1 expression and down-regulated NF-κB p-p65 expression in AR42J cells in the HTG environment. When treated with SC75741, an inhibitor of the

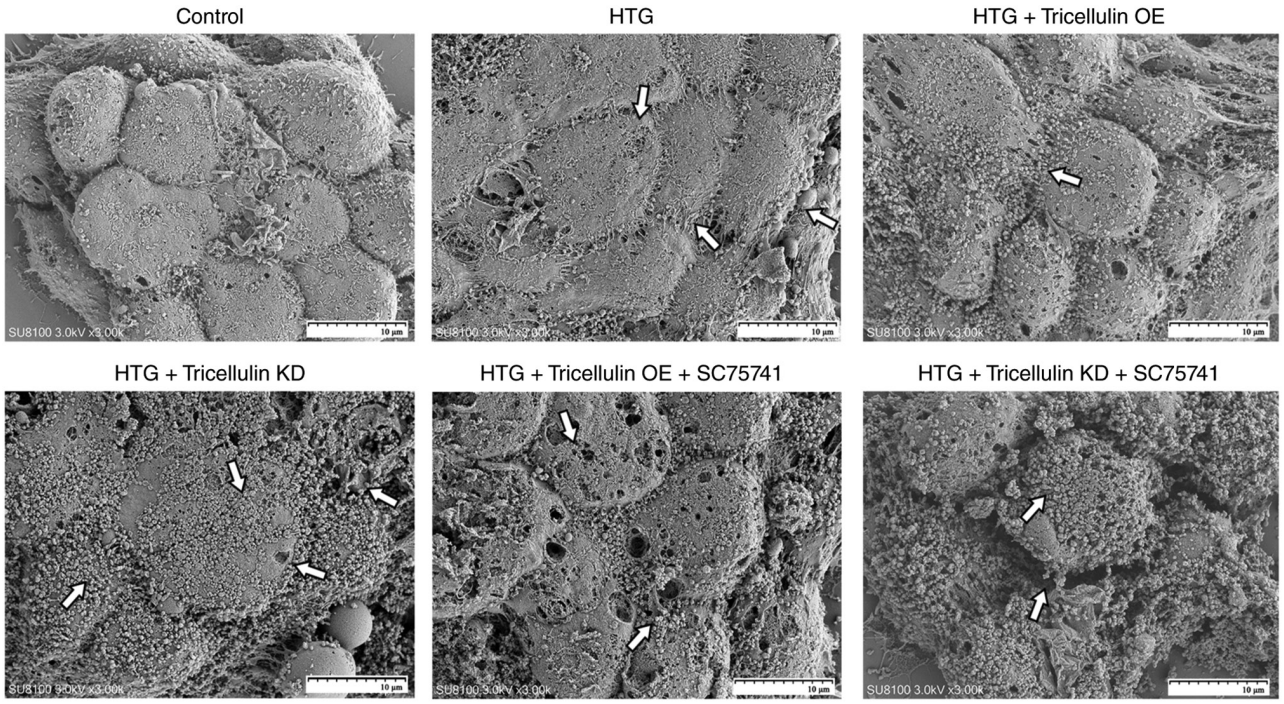

Figure 5. Representative images of scanning electron microscopic analysis of intercellular morphology and cell-cell contacts in AR42J cells under HTG conditions and SC75741 treatment. White arrows indicate representative changes including cell swelling, surface irregularity and weakened cell-cell contacts. Scale bars, 10 μm. HTG, hypertriglyceridemia; KD, knockdown; NC, negative control; OE, overexpression.

NF-κB pathway, the expression levels of NF-κB p-p65 further decreased, whereas those of tricellulin and claudin-1 increased. Conversely, knockdown of tricellulin downregulated claudin-1 expression and upregulated NF-κB p-p65 expression in AR42J cells in the HTG environment. SC75741 treatment inhibited NF-κB activation, and was associated with partial recovery of tricellulin and claudin-1 expression compared with the corresponding groups without SC75741 treatment.

Effects of tricellulin on F-actin dynamics in AR42J cells in the HTG environment and treated with SC75741. Immunofluorescence was performed to analyze how the regulation of tricellulin and treatment with SC75741 impacted F-actin dynamics. Under HTG conditions, the F-actin network showed reduced continuity, weaker cortical distribution and a more disorganized filament pattern compared with the control group (Fig. 4). Tricellulin overexpression was associated with partial restoration of F-actin organization, whereas tricellulin knockdown was associated with more pronounced disruption. These changes remained evident after SC75741 treatment.

*Effects of tricellulin on cell surface morphology and intercellular contacts in AR42J cells in the HTG environment and treated with SC75741. R*epresentative scanning electron micrographs showed that control cells were regularly arranged with relatively intact intercellular contacts and smooth surfaces (Fig. 5). Under HTG conditions, cells showed swelling, membrane injury and weakened cell-cell contacts. These changes appeared less pronounced in the tricellulin overexpression group and more severe in the tricellulin knockdown group. Following SC75741 treatment, cellular damage remained evident, particularly in the tricellulin knockdown group.

Discussion

HTG is increasingly recognized not only as a metabolic abnormality but also as a pro-inflammatory state that may sensitize pancreatic tissue to injury. In the present study, *in vivo* and *in vitro* models were used to investigate the potential role of tricellulin in pancreatic injury under hypertriglyceridemic conditions. The findings showed that hypertriglyceridemic conditions were associated with reduced tricellulin expression, increased NF-κB pathway activation, impaired TJ-related protein expression, specifically reduced tricellulin and claudin-1 expression, and cytoskeletal disorganization. In the hamster model, HTGAP was accompanied by markedly aggravated pancreatic injury, decreased tricellulin and claudin-1 expression, and increased p65 expression. In AR42J cells, tricellulin overexpression was associated with increased claudin-1 expression, reduced NF-κB activation, improved F-actin organization and better-preserved intercellular morphology, whereas tricellulin knockdown showed the opposite pattern. Together, the observed reductions in tricellulin and claudin-1 expression, the increase in NF-κB activation, and the disruption of F-actin organization support the potential role of tricellulin in HTGAP-related TJ and cytoskeletal injury.

Although mice and rats are the most commonly used models for pancreatitis, their disease characteristics may not compare to those of human diseases, particularly with respect to lipid metabolism (29). Hamsters have been used as a relevant model in pancreatic disease research (30,31) and are capable of developing a relatively stable hypertriglyceridemic state that more closely resembles the human metabolic condition. Some studies have shown that elevated

TGs could cause the cells to remain in a state of low-grade inflammation, leading to persistent oxidative stress, endothelial system dysfunction, insulin resistance and intestinal flora imbalance (32,33).

In the present study, HTG alone was associated with reduced tricellulin expression and mildly increased p65 expression, whereas no significant increase in pancreatic histopathological injury was observed in the HTG group *in vivo*. By contrast, under HTG-like conditions *in vitro*, pancreatic acinar cells showed decreased tricellulin and claudin-1 expression, increased NF-κB activation, disrupted F-actin organization, weakened intercellular contacts and more evident membrane injury than control cells. These changes suggest that HTG may create a vulnerable background characterized by low-grade inflammatory activation and junctional instability. Mild-to-moderate elevations in pancreatic TG levels may therefore not directly cause marked acinar necrosis, but may aggravate and amplify the inflammatory susceptibility of acinar cells in the presence of an additional injurious stimulus (34).

Patients with HTG-induced AP experience a worse prognosis compared with patients in whom this condition was triggered by other causes (35). In the present study, hamsters in the HTGAP group showed markedly more severe pancreatic injury than those in the control and HTG groups. In parallel, tricellulin and claudin-1 expression in pancreatic tissues was significantly decreased, whereas p65 expression was significantly increased. After treatment with SC75741, pancreatic injury and p65 expression were significantly decreased, whereas tricellulin and claudin-1 showed only partial recovery compared with the untreated HTGAP group. These findings support the involvement of NF-κB signaling in HTGAP-related pancreatic injury, while also suggesting that changes in TJ-related proteins may be associated with, rather than definitively opposed to, NF-κB pathway activation in this setting.

TJ disruption may be one mechanism contributing to this process. Tricellulin is a key component of tTJs and is essential for epithelial barrier maintenance. Previous studies have mainly focused on tricellulin or TJ alterations in epithelial barriers, pancreatic ductal cells or other disease contexts (9,36), whereas less attention has been paid to pancreatic acinar cells under hypertriglyceridemic conditions. The present findings extend this area by showing that tricellulin expression was already reduced in the HTG group and further decreased in the HTGAP group, suggesting that metabolic stress may precede and intensify junctional injury. In addition, tricellulin modulation in AR42J cells was accompanied by corresponding changes in claudin-1 expression and intercellular morphology, supporting the possibility that tricellulin participates in maintaining junctional homeostasis in pancreatic acinar cells during HTGAP-related injury.

Tricellulin is one of the main constituents of TJ formation and is primarily localized at tTJs (37). Previous studies on tricellulin have mainly been conducted in the field of oncology, where altered tricellulin expression has been associated with tumor behavior and differentiation (17,37). By contrast, to the best of our knowledge, little is known about the relationship between tricellulin and inflammatory signaling in HTGAP. In the current *in vitro* experiments, tricellulin overexpression was associated with increased claudin-1 expression and reduced NF-κB activation under HTG-like condition, whereas tricellulin knockdown showed the opposite pattern. These findings suggested that tricellulin may contribute to the regulation of junctional integrity in pancreatic acinar cells and could be linked to inflammatory signaling changes involving NF-κB. However, the present results do not establish a direct molecular interaction between tricellulin and the NF-κB pathway.

NF-κB signaling is one of the central inflammatory pathways implicated in AP, and has also been linked to junctional remodeling and cytoskeletal regulation in other biological settings (20,21). In the present study, p65 expression was significantly increased in the HTGAP group and remained elevated in the HTGAP + SC75741 group compared with that in the control group, although it was significantly reduced after SC75741 treatment compared with the untreated HTGAP group. These findings support the involvement of NF-κB signaling in HTGAP-associated pancreatic injury. Although p-p65 more directly reflects NF-κB activation, the modest variation in total p65 may reflect concurrent changes in overall p65 protein abundance across the groups. However, the interpretation should remain cautious. Although SC75741 significantly reduced histopathological injury and p65 expression, tricellulin and claudin-1 expression showed only partial recovery and did not differ significantly between the HTGAP and HTGAP + SC75741 groups. Therefore, the present data support a potential association between tricellulin-related changes and NF-κB activation, but do not establish a direct molecular interaction or a fully defined causal pathway.

The cytoskeleton is a special network structure composed of multiple protein filaments, polymerized and intertwined intercellularly. These protein filaments exhibit a dynamic balance under the action of various regulatory factors to maintain the integrity and stability of cell morphology and structure, facilitate the transport of intracellular substances and the stable movement of organelles, and participate in cell deformation and cell division (19,38). F-actin, a type of cytoskeletal protein filament, is formed by the spiral intercalated polymerization of actin molecules (39). They utilize the energy of actin polymerization, interact with myosin II, and serve an important role in the formation of cell membranes and the secretion of intracellular substances (40). After acinar cells are stimulated by cholecystokinin, myosin II, which is dependent on the G protein-coupled receptor signaling pathway, is phosphorylated and redistributed to the outside of the basement membrane, increasing the cell membrane tension there, prompting the formation of vesicles rich in zymogen granules and their secretion outward. Multiple signaling pathways participate in regulating the functions of microfilaments and the cytoskeleton, such as FAK, ROCK/NF-κB, PI3K and MAPK (20,29).

In the present study, the HTG-like condition disrupted the F-actin network and weakened cell-cell contacts, whereas tricellulin overexpression was associated with partial restoration of F-actin organization and intercellular morphology. Conversely, tricellulin knockdown further aggravated cytoskeletal disorganization and junctional damage. These findings support a possible link between tricellulin, junctional stability and cytoskeletal organization under hypertriglyceridemic stress.

The current study has several limitations. First, the sample size in the animal experiments was relatively small, and no formal *a priori* power calculation was performed; therefore, the findings should be considered exploratory. Second, only female hamsters were used, and no direct comparison between sexes was performed, thus sex-specific differences could not be assessed. Third, only one animal model and one rat-derived acinar cell line were used, which may limit generalizability. Fourth, sham-operated controls were not included. Fifth, although changes in NF-κB signaling were observed after tricellulin modulation and SC75741 treatment, the present study did not directly verify the molecular interaction between tricellulin and the NF-κB pathway, nor could it exclude potential off-target effects of pharmacological inhibition. Finally, neither human pancreatic tissues nor a clinical validation cohort were available to support the translational relevance of the findings. Future studies should include larger experimental cohorts, additional model systems, direct mechanistic assays and validation in human samples.

In conclusion, the present study suggested that hypertriglyceridemic conditions may be associated with impaired TJ integrity and cytoskeletal organization in pancreatic acinar cells. Tricellulin may contribute to this process and could be linked to inflammatory signaling changes involving NF-κB. These findings provide a basis for further mechanistic investigation of epithelial junctional injury in HTGAP.

Acknowledgment

Not applicable.

Funding

The present study was funded by the Joint Project on Regional High-Incidence Diseases Research of Guangxi Natural Science Foundation (grant nos. 2023GXNSFAA026455 and 2024GXNSFAA010406) and the Chinese National Natural Science Foundation (grant no. 82360135).

Availability of data and materials

The data generated in the present study may be requested from the corresponding author.

Authors' contributions

GW, ZheL and HW drafted the manuscript. MQ conceived the study. GW, ZheL, HW, QW and LL performed the experiments. JW, HY and ZhiL analyzed the data. ZhiL and MQ revised the manuscript. GW and MQ confirm the authenticity of all the raw data. All authors read and approved the final manuscript.

Ethics approval and consent to participate

The present study was approved by the Ethics Committee for Medical Experimental Animals, Second Affiliated Hospital of Guangxi Medical University [approval no. 2022(KY-0174)].

Patient consent for publication

Not applicable.

Competing interests

The authors declare that they have no competing interests.

References

1. Jin M, Bai X, Chen X, Zhang H, Lu B, Li Y, Lai Y, Qian J and Yang H: A 16-year trend of etiology in acute pancreatitis: The increasing proportion of hypertriglyceridemia-associated acute pancreatitis and its adverse effect on prognosis. J Clin Lipidol 13: 947-953.e1, 2019.
2. Mederos MA, Reber HA and Girgis MD: Acute pancreatitis: A review. JAMA 325: 382-390, 2021.
3. Wan J, He W, Zhu Y, Zhu Y, Zeng H, Liu P, Xia L and Lu N: Stratified analysis and clinical significance of elevated serum triglyceride levels in early acute pancreatitis: A retrospective study. Lipids Health Dis 16: 124, 2017.
4. Adiamah A, Psaltis E, Crook M and Lobo DN: A systematic review of the epidemiology, pathophysiology and current management of hyperlipidaemic pancreatitis. Clin Nutr 37 (6 Pt A): 1810-1822, 2018.
5. Vlacho B, Julve J, Genua I, Fernández-Camins B, Real J, Franch-Nadal J, Mauricio D and Ortega E: Hypertriglyceridemia and its relationship with all-cause mortality and pancreatitis: Results from a large retrospective clinical registry. J Clin Lipidol 19: 922-930, 2025.
6. Zheng J, Wu J, Chen J, Liu J, Lu Y, Huang C, Hu G, Wang X and Zeng Y: Therapeutic effects of quercetin on early inflammation in hypertriglyceridemia-related acute pancreatitis and its mechanism. Pancreatology 16: 200-210, 2016.
7. Yang AL and McNabb-Baltar J: Hypertriglyceridemia and acute pancreatitis. Pancreatology 20: 795-800, 2020.
8. Slifer ZM and Blikslager AT: The integral role of tight junction proteins in the repair of injured intestinal epithelium. Int J Mol Sci 21: 972, 2020.
9. Wang J, Qin M, Wu Q, Yang H, Wei B, Xie J, Qin Y, Liang Z and Huang J: Effects of lipolysis-stimulated lipoprotein receptor on tight junctions of pancreatic ductal epithelial cells in hypertriglyceridemic acute pancreatitis. Biomed Res Int 2022: 4234186, 2022.
10. Furuse M, Izumi Y, Oda Y, Higashi T and Iwamoto N: Molecular organization of tricellular tight junctions. Tissue Barriers 2: e28960, 2014.
11. Zihni C, Mills C, Matter K and Balda MS: Tight junctions: From simple barriers to multifunctional molecular gates. Nat Rev Mol Cell Biol 17: 564-580, 2016.
12. Higashi T and Miller AL: Tricellular junctions: How to build junctions at the TRICkiest points of epithelial cells. Mol Biol Cell 28: 2023-2034, 2017.
13. Morampudi V, Graef FA, Stahl M, Dalwadi U, Conlin VS, Huang T, Vallance BA, Yu HB and Jacobson K: Tricellular tight junction protein tricellulin is targeted by the enteropathogenic escherichia coli effector EspG1, leading to epithelial barrier disruption. Infect Immun 85: e00700-16, 2017.
14. Weber CR, Raleigh DR, Su L, Shen L, Sullivan EA, Wang Y and Turner JR: Epithelial myosin light chain kinase activation induces mucosal interleukin-13 expression to alter tight junction ion selectivity. J Biol Chem 285: 12037-12046, 2010.
15. Oda Y, Otani T, Ikenouchi J and Furuse M: Tricellulin regulates junctional tension of epithelial cells at tricellular contacts through Cdc42. J Cell Sci 127 (Pt 19): 4201-4212, 2014.
16. Schuetz A, Radusheva V, Krug SM and Heinemann U: Crystal structure of the tricellulin C-terminal coiled-coil domain reveals a unique mode of dimerization. Ann N Y Acad Sci 1405: 147-159, 2017.
17. Korompay A, Borka K, Lotz G, Somorácz A, Törzsök P, Erdélyi-Belle B, Kenessey I, Baranyai Z, Zsoldos F, Kupcsulik P, *et al*: Tricellulin expression in normal and neoplastic human pancreas. Histopathology 60 (6B): E76-E86, 2012.

18. Yang HY, Liang ZH, Xie JL, Wu Q, Qin YY, Zhang SY and Tang GD: Gelsolin impairs barrier function in pancreatic ductal epithelial cells by actin filament depolymerization in hypertriglyceridemia-induced pancreatitis in vitro. Exp Ther Med 23: 290, 2022.
19. Yang D, Yang L, Cai J, Li H, Xing Z and Hou Y: Phosphoinositide 3-kinase/Akt and its related signaling pathways in the regulation of tumor-associated macrophages polarization. Mol Cell Biochem 477: 2469-2480, 2022.
20. Zhang X, Yang G, Chen Y, Mu Z, Zhou H and Zhang L: Resveratrol pre-treatment alleviated caerulein-induced acute pancreatitis in high-fat diet-feeding mice via suppressing the NF-κB proinflammatory signaling and improving the gut microbiota. BMC Complement Med Ther 22: 189, 2022.
21. Guan G, Cannon RD, Coates DE and Mei L: Effect of the Rho-Kinase/ROCK Signaling pathway on cytoskeleton components. Genes (Basel) 14: 272, 2023.
22. Zhang JX, Qin MB, Ye Z, Peng P, Li SM, Song Q, Lin L, Liu SQ, Xie LH, Zhu Y and Huang JA: Association of tricellulin expression with poor colorectal cancer prognosis and metastasis. Oncol Rep 44: 2174-2184, 2020.
23. Oh SS and Narver HL: Mouse and rat anesthesia and analgesia. Curr Protoc 4: e995, 2024.
24. Zhang LG, Yu ZQ, Yang C, Chen J, Zhan CS, Chen XG, Zhang L, Hao ZY and Liang CZ: Effect of Eriocalyxin B on prostatic inflammation and pelvic pain in a mouse model of experimental autoimmune prostatitis. Prostate 80: 1394-1404, 2020.
25. Pang D and Laferriere C: Review of intraperitoneal injection of sodium pentobarbital as a method of euthanasia in laboratory rodents. J Am Assoc Lab Anim Sci 59: 346, 2020.
26. Zatroch KK, Knight CG, Reimer JN and Pang DS: Refinement of intraperitoneal injection of sodium pentobarbital for euthanasia in laboratory rats (Rattus norvegicus). BMC Vet Res 13: 60, 2017.
27. Van Laethem JL, Marchant A, Delvaux A, Goldman M, Robberecht P, Velu T and Devière J: Interleukin 10 prevents necrosis in murine experimental acute pancreatitis. Gastroenterology 108: 1917-1922, 1995.
28. Livak KJ and Schmittgen TD: Analysis of relative gene expression data using real-time quantitative PCR and the 2(-Delta Delta C(T)) Method. Methods 25: 402-408, 2001.
29. Lerch MM and Gorelick FS: Models of acute and chronic pancreatitis. Gastroenterology 144: 1180-1193, 2013.
30. Miao J, Kang L, Lan T, Wang J, Wu S, Jia Y, Xue X, Guo H, Wang P and Li Y: Identification of optimal reference genes in golden Syrian hamster with ethanol- and palmitoleic acid-induced acute pancreatitis using quantitative real-time polymerase chain reaction. Animal Model Exp Med 6: 609-618, 2023.
31. Cai W, Bhattacharya P, Li Y, Wen Y, Shi N, Liu T, Xia Q, Sutton R, Huang W and Mukherjee R: Circulating cyclophilin A levels elevate in animal models and can predict mortality in patients with acute pancreatitis. Pancreatology 25: 301-306, 2025.
32. Hutchinson AN, Tingo L and Brummer RJ: The potential effects of probiotics and omega-3 fatty acids on chronic low-grade inflammation. Nutrients 12: 2402, 2020.
33. Zhu L, Guo L, Xu J, Xiang Q, Tan Y, Tian F, Du X, Zhang S, Wen T and Liu L: Postprandial triglyceride-rich lipoproteins-induced lysosomal dysfunction and impaired autophagic flux contribute to inflammation in white adipocytes. J Nutr 154: 1619-1630, 2024.
34. Park CH, Chung MJ, Park DH, Min S and Park SW: Impact of pancreatic fat on the risk of post-endoscopic retrograde cholangiopancreatography pancreatitis. Surg Endosc 36: 5734-5742, 2022.
35. Fan Z, Zhang Y, Li J, He W, Bai X, Cai Y, Li N, Xie F, Wen L, Akshintala VS, *et al*: Global burden and characterization of hypertriglyceridemia-induced acute pancreatitis: Results from a systematic review and a multi-center cohort study. Sci China Life Sci 68: 3010-3020, 2025.
36. Raleigh DR, Marchiando AM, Zhang Y, Shen L, Sasaki H, Wang Y, Long M and Turner JR: Tight junction-associated MARVEL proteins marveld3, tricellulin, and occludin have distinct but overlapping functions. Mol Biol Cell 21: 1200-1213, 2010.
37. Kojima T, Takasawa A, Kyuno D, Ito T, Yamaguchi H, Hirata K, Tsujiwaki M, Murata M, Tanaka S and Sawada N: Downregulation of tight junction-associated MARVEL protein marvelD3 during epithelial-mesenchymal transition in human pancreatic cancer cells. Exp Cell Res 317: 2288-2298, 2011.
38. Umbayev B, Saliev T, Safarova Yantsen Y, Yermekova A, Olzhayev F, Bulanin D, Tsoy A and Askarova S: The role of Cdc42 in the insulin and leptin pathways contributing to the development of age-related obesity. Nutrients 15: 4964, 2023.
39. Castaneda N, Park J and Kang EH: Regulation of actin bundle mechanics and structure by intracellular environmental factors. Front Phys 9: 675885, 2021.
40. Chakrabarti R, Lee M and Higgs HN: Multiple roles for actin in secretory and endocytic pathways. Curr Biol 31: R603-R618, 2021.